Initial three-dimensional finite-difference time-domain phenomenology study of the transient response of a large vertically coupled photonic racetrack

Jethro H. Greene and Allen Taflove

Department of Electrical and Computer Engineering, Northwestern University, 2145 Sheridan Road, Evanston, Illinois 60208

Received March 31, 2003

We report the initial three-dimensional finite-difference time-domain modeling of a vertically coupled photonic racetrack. The modeling reveals details of the full suite of space–time behavior of electromagnetic-wave phenomena involved in guiding, coupling, multimoding, dispersion, and radiation. This behavior is not easily obtainable by analytical or full-vector frequency-domain methods, measurements of terminal properties, or near-field scanning optical microscopy. © 2003 Optical Society of America

OCIS codes: 230.3120, 230.5750, 230.7370.

The finite-difference time-domain (FDTD) solution method for Maxwell's equations has been extensively applied to model and design microwave and photonic devices and circuits.[1] FDTD models of waveguiding photonic devices have used the effective refractive-index approximation to reduce large-scale three-dimensional (3-D) simulations to computationally tractable two-dimensional (2-D) problems. Relevant examples include reported FDTD models of micrometer-scale rings, racetracks, and disk resonators of various shapes.[1–4] However, the very nature of 2-D modeling prevents simulation of the important class of guided-wave photonic structures wherein the waveguide-to-resonator coupling occurs in the vertical direction rather than sideways in the plane of the resonator.

Recent progress in parallel computing now permits direct full-wave FDTD modeling of 3-D photonic devices and circuits. In this regard, this Letter reports the formulation and results of what we believe to be the first fully 3-D FDTD model of vertical waveguide coupling and subsequent optical beam confinement in a photonic racetrack. The present work extends to the vertical coupling case previous efforts that used 2-D FDTD modeling to obtain the phenomenology of sideways coupling.[1,2] Furthermore, this Letter points the way toward routine usage of 3-D FDTD modeling for designing large, complex, micro-optical circuits. Such modeling can reveal the full suite of space–time behavior of electromagnetic-wave phenomena involved in guiding, coupling, multimoding, dispersion, and radiation, which is not easily obtainable by analytical or full-vector frequency-domain methods,[5] measurements of device terminal properties, or near-field scanning optical microscopy.[6]

Referring to Figs. 1 and 2, we note that the geometry considered here consists of a straight bus waveguide located 1.343 μm below and parallel to one of the straight sections of a photonic racetrack that spans 64.0 μm $\times$ 17.6 μm. Figure 1 shows the $x-y$ planes containing the bus waveguide and the racetrack, and Fig. 2 shows the $y-z$ plane cross section at P_2, the center of one of the straight sections of the racetrack. The bus waveguide consists of a 2.015 μm $\times$ 0.775 μm rectangular cross-section channel of refractive index $n = 3.33$ embedded within a uniform substrate of index $n = 3.17$. The racetrack consists of a 2.015 μm $\times$ 0.775 μm rectangular cross-section channel of refractive index $n = 3.33$ sandwiched above and below by rectangular cross-section channels of refractive index $n = 3.17$, all embedded within a uniform superstrate of index $n = 1.5$.

By use of the bootstrapping technique,[1] the straight bus waveguide is excited in its fundamental TE mode with a numerical Gaussian pulsed source having a center free-space wavelength $\lambda_0 = 2.32$ μm. Because the bootstrapping runs indicate 3- and 1.5-μm λ_0 cutoffs for the fundamental and the first higher-order modes, respectively, the source spectrum is adjusted to span $2.17 < \lambda_0 < 2.47$ μm (full width at half-maximum) to avoid multimoding in the straight waveguide.

Wideband spectral responses are obtained with only a single FDTD run by use of concurrent discrete Fourier transformations of calculated field-versus-time waveforms[1] at the key transverse cross sections P_1 through P_4 in Fig. 1. This permits calculating as a

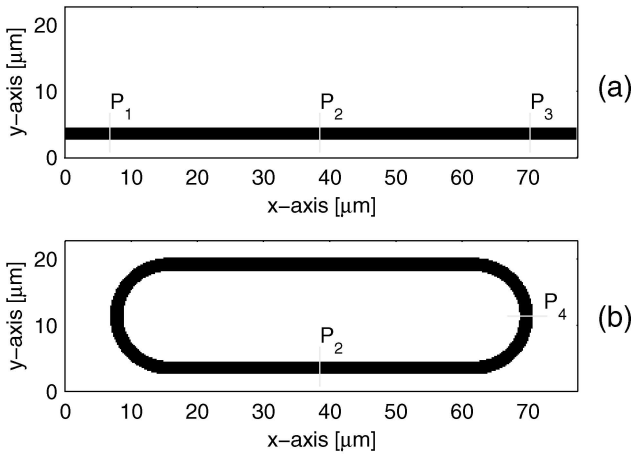

Fig. 1. Horizontal ($x-y$) cuts through the 3-D FDTD modeling geometry: (a) through the bus waveguide beneath the racetrack, (b) through the racetrack. Vertical transverse field observation cut planes P_1, P_2, P_3, and P_4 are also shown.

0146-9592/03/191733-03$15.00/0

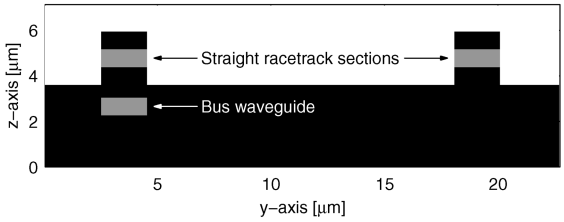

Fig. 2. Vertical (y–z) cross section through the 3-D FDTD modeling geometry at P_2 in the center of the coupling region.

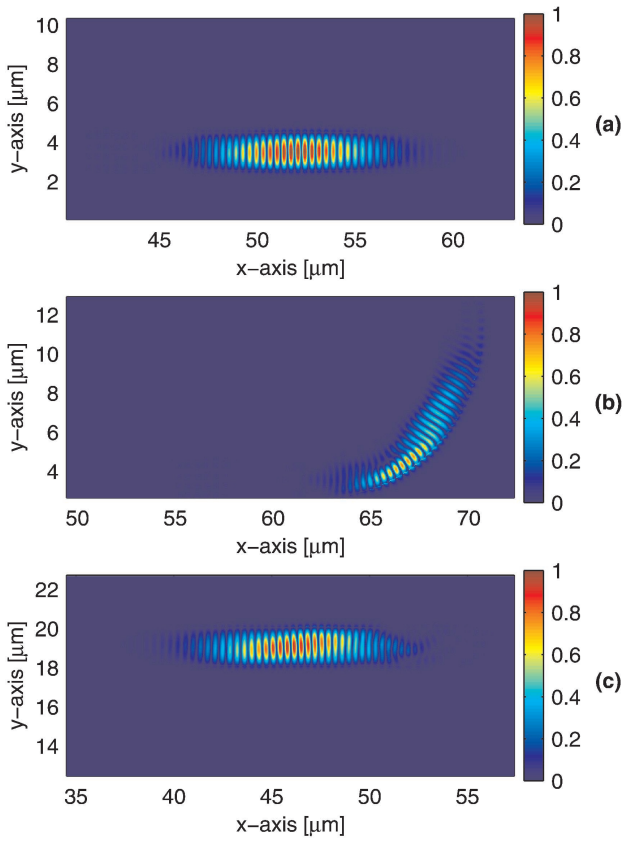

Fig. 3. FDTD-calculated absolute value of the y component of the electric field of the optical pulse within the racetrack: (a) $+x$-directed propagation immediately after the initial coupling from the bus waveguide; (b) counterclockwise propagation upon entering the first curved section, showing modal distortion; (c) $-x$-directed propagation after exiting the first curved section, showing residual modal-distortion effects.

function of frequency the magnitude and phase of the corresponding time-harmonic transverse fields, the local Poynting vectors, and the integrated optical power flow. In turn, this calculation yields the broadband spectral characterization of the coupling efficiency, η (the total power flow through P_4 normalized by the incident power flow through P_1); the transmittance, τ (the normalized power flow through P_3), and the round-trip racetrack power retention ratio, ρ. Here, η includes the effect of the radiation loss that occurs at the beginning of the colocation of the bus and racetrack waveguides; τ is obtained with the discrete Fourier transform temporal window narrowed to exclude backcoupling from the racetrack to the bus waveguide; and ρ includes the effect of losses that are due to radiation as well as backcoupling to the bus waveguide.

We apply the standard Yee-based FDTD method[1] to a uniform $1500 \times 440 \times 138$-cell Cartesian cubic mesh of resolution 51.7 nm ($\lambda_0/45$ at the center wavelength of 2.32 μm). A 12-cell uniaxial perfectly matched layer absorbing boundary condition[1] is used to terminate the FDTD mesh with wave reflections below 0.01%. The simulation is run on a Cray T3E with 125 distributed-memory processors coupled with Cray's implementation of the message passing interface standard.

Figure 3 provides pseudo-color visualizations of the absolute value of the FDTD-calculated y component of the optical electric field within the racetrack at three key points: (1) in the vicinity of P_2 immediately after coupling from the bus waveguide, showing the

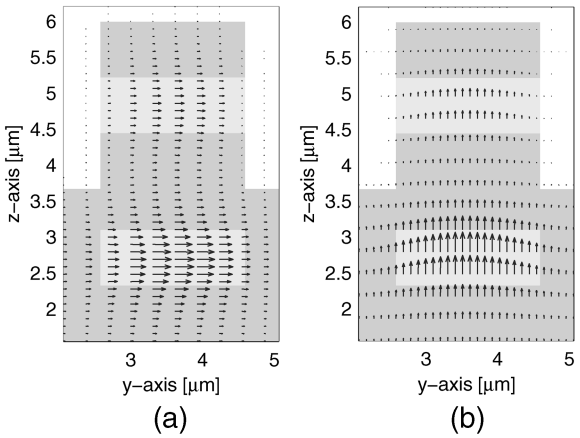

Fig. 4. FDTD-calculated transverse field vectors in the vertical (y–z) cross section at P_2 at the instant of peak excitation within the bus waveguide: (a) electric field E, (b) magnetic field H. The bus and racetrack waveguides are shown as shaded rectangles.

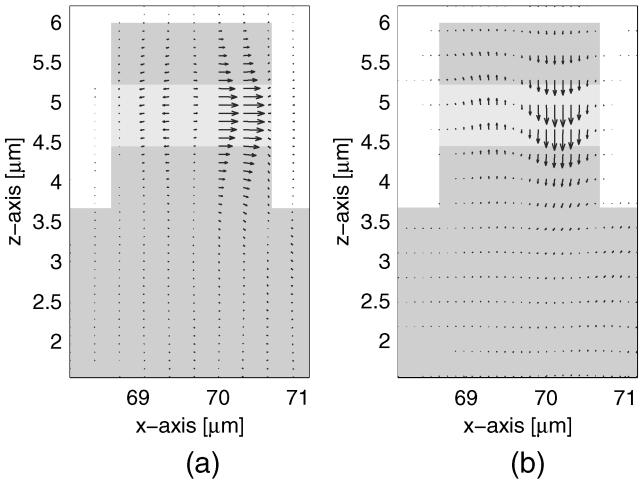

Fig. 5. FDTD-calculated transverse field vectors in the vertical (x–z) cross section at P_4 at the instant of peak excitation within the racetrack waveguide: (a) electric field E, (b) magnetic field H. The racetrack waveguide is shown as a shaded rectangle.

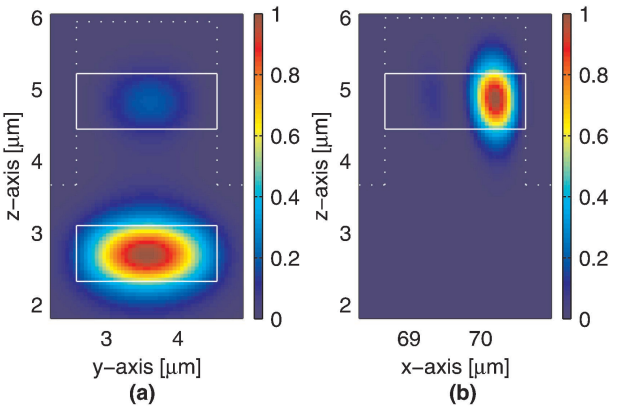

Fig. 6. Relative FDTD-calculated Poynting vector in the direction of propagation. The magnitudes are normalized by the maximum magnitude in each plot, and the boundaries of the bus and racetrack waveguides are shown as solid rectangles. (a) x component of the Poynting vector along the vertical ($y-z$) cross section at P_2 at the instant of peak excitation within the bus waveguide, (b) y component of the Poynting vector along the vertical ($x-z$) cross section at P_4 at the instant of peak excitation within the racetrack waveguide.

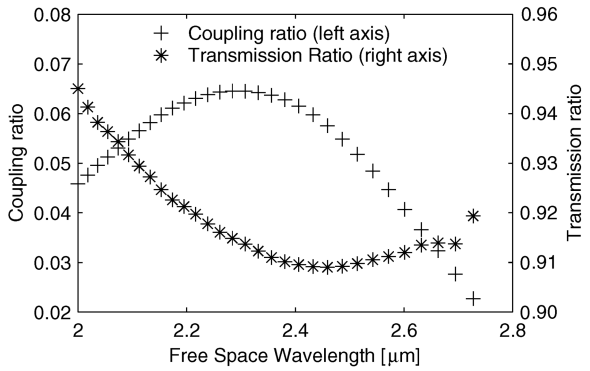

Fig. 7. FDTD-calculated ratio of the coupled racetrack power at P_4 to the incident bus waveguide power as a function of wavelength (left axis) and FDTD-calculated ratio of the transmitted bus waveguide power to the incident bus waveguide power as a function of wavelength (right axis). Subsequent backcouplings from the racetrack to the bus waveguide are excluded.

establishment of the fundamental propagating mode; (2) approaching P_4 in the first curved section, showing the onset of multimoding; and (3) after exiting the first curved section, showing residual modal-distortion effects and pulse dispersion. Figures 4–6 provide visualizations of the corresponding transverse field vectors and longitudinal Poynting vector in the vertical cross sections at P_2 and P_4. These figures show that transient multimoding arises within the curved section. This multimoding spatially distorts the propagating optical pulse both by longitudinally broadening it and by shifting its local power flow toward the outer curved waveguide boundary.

Figure 7 graphs the coupling efficiency, η, and transmittance, τ, versus wavelength. The midband value of η can be seen to be the maximum, ~6.5%, dropping to ~4.5% at $\lambda_0 = 2.1$ μm and ~2.3% at $\lambda_0 = 2.7$ μm. Figure 8 shows the round-trip racetrack power retention ratio, ρ, as observed at P_4. We note that ρ doubles from ~37% at $\lambda_0 = 2.7$ μm to ~75% upon approaching $\lambda_0 = 2$ μm but then begins to fall despite decreasing backcoupling to the bus waveguide and increasing field confinement within the racetrack's straight sections. On the basis of Figs. 3–6, we believe that this behavior of ρ is caused by increased radiation from the racetrack's curved sections as a result of transient multimoding that shifts the optical power toward the outer waveguide boundary, where surface roughness can help to launch freely propagating energy.

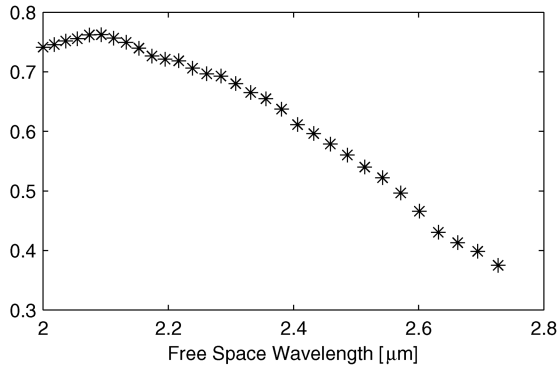

Fig. 8. FDTD-calculated power retention within the racetrack as a function of wavelength. A single complete propagation around the racetrack from P_4 back to P_4 is considered.

Work is ongoing to use 3-D FDTD modeling to develop corresponding phenomenology for the orthogonal z-polarized TE bus waveguide mode and to develop quantitative data for resonant frequencies, Q factors, and free spectral ranges for both the y- and z-polarized TE bus waveguide modes.

The authors thank Cray Research, Inc., for their generous grant of Cray T3E supercomputer resources. We acknowledge the partial support of this work by Princeton Lightwave, Inc., and the suggestion of the problem geometry by Giora Griffel of Princeton Lightwave. J. H. Greene's e-mail address is jhgreen@northwestern.edu.

References

1. A. Taflove and S. C. Hagness, *Computational Electrodynamics: The Finite-Difference Time-Domain Method*, 2nd ed. (Artech House, Norwood, Mass., 2000).
2. S. C. Hagness, D. Rafizadeh, S. T. Ho, and A. Taflove, J. Lightwave Technol. **15,** 2154 (1997).
3. A. Sakai and T. Baba, J. Lightwave Technol. **17,** 1493 (1999).
4. W.-H. Guo, Y.-Z. Huang, and Q.-M. Wang, IEEE Photon. Technol. Lett. **12,** 813 (2000).
5. B. E. Little and S. T. Chu, IEEE Photon. Technol. Lett. **12,** 401 (2000).
6. G. H. Vander Rhodes, B. B. Goldberg, M. S. Unlu, S.-T. Chu, and B. E. Little, IEEE J. Sel. Top. Quantum Electron. **6,** 46 (2000).